Effect of mechanical support conditions of winding on the strain development of a composite MgB₂ based full body MRI coil

A. A. Amin, T. N. Baig, R. J. Deissler, L. Sabri, D. Doll, M. Tomsic, O. Akkus and M. A. Martens

Abstract— **The winding of composite superconducting wire around a mandrel is one of the first stages of manufacturing processes of a superconducting magnet. Depending on the method of mechanical support conditions during winding, the strain development at the final stage in a superconducting magnet may vary significantly. Therefore, proper selection of the winding process is important to increase the feasibility for a conduction cooled full body MRI magnet based on magnesium diboride (MgB₂), a strain sensitive high temperature (HTS) superconductor. A multiscale multiphysics Finite Element Analysis (FEA) model of an 18 filament MgB₂ wire is developed for strain estimation. The computationally homogenized representative volume element (RVE) of the composite wire is used in the coil bundle in place of the actual MgB₂ wire. The simulation considers winding, thermal cool-down and electromagnetic charging to estimate total strain developed at the final step— electromagnetic charging. Four different types of support conditions are studied and strain development is reported. Results suggest that a combination of radial and axial support at the inner radial surface and outermost axial surfaces of the mandrel respectively is the most favorable winding condition with a minimum strain development of 0.021% which is half in comparison to no mandrel support.**

Index Terms— **Finite Element Analysis, ANSYS, Superconducting Coils, MRI, Multiphysics, Multiscale modeling.**

I. INTRODUCTION

HIGH temperature superconductors such as MgB₂ show promise for conduction cooled magnetic resonance imaging (MRI) machines, operating at temperatures higher than the boiling point of liquid helium (LHe). However, a conductively cooled full body MRI magnet is yet to be devised. Previously, optimized electromagnetic design of 1.5 T and 3.0 T conduction cooled MgB₂ magnet has been presented by Baig et. al. [1]. Nevertheless, mechanical design aspects addressing the strain sensitivity of MgB₂ remain a major concern as experimental testing of composite wire confirms the operating limitation beyond strain values of -0.6% to 0.4% [2]–[5], a value much lower in comparison to Nb-Ti strain limit of 1% [6]. Such a narrow design limit prompts a careful computational

analysis preceding the actual manufacturing process. Unfortunately, straight forward finite element analysis (FEA) or any other computational approach requires the material properties of the composite superconducting wire, which in most cases are unavailable because of the extensive experimentation needed to attain them. However, with the help of multiscale modeling and the use of available basic material property data of the constituent composite wire, it is possible to approximate the material behavior of a representative volume element (RVE) of a composite wire. Stepping up from the wire length scale to the bundle length scale allows one to analyze the full MRI magnet system for strain development. The analysis of the manufacturing and electromagnetic operation— utilizing the RVE properties, requires the interaction between several different fields of physics— elasticity and electromagnetics. Hence, the problem turns into multiscale-multiphysics where different physics fields interact with each other at different length scales.

The mechanical support conditions during winding have been studied before [7] for NbTi based magnet. It is shown that the floating coil technique[8] helps in reducing the possibility of a quench [9] by eliminating local conductor motion and thus reducing shear stresses [7], [10]. Similar studies are necessary for the system in consideration to check the feasibility of a full body 1.5 T magnet system due to the high strain sensitivity of MgB₂. However, conduction cooling system restricts the use of floating coil technique as the technique would degrade conduction performance. The proposed system has been optimized for second generation MgB₂ wire according to methods detailed by Baig et al. [1] and summarized in prior articles [11], [12]. Quench propagation system was analyzed by Poole et al. [11] and protection systems was studied by Deissler et al. [13] in previous studies. Strain development in MgB₂ for the system has been considered in prior work [14]. However, computational study regarding various winding processes would help the manufacturer choose among the most favorable winding techniques— allowing more room for a quench protection system regarding failure stress and strains, and

A. A. Amin, L. Sabri and O. Akkus is with the Case Western Reserve University Department of Mechanical and Aerospace Engineering, OH 44106 USA. (e-mail: aaa196@case.edu).

D. Doll and M. Tomsic is with the Hypertech Research, Columbus OH 43228 USA

T. N. Baig, R. J. Deissler, and M. A. Martens are with Case Western Reserve University Department of Physics, OH 44106 USA.

would eventually result in a much robust design. Therefore, to analyze the effect of mechanical support conditions in this study, a 1.5 T full body MRI magnet system is considered and studied using a multiscale multiphysics approach based on FEA in ANSYS.

II. MATERIALS AND METHODS

A. 1.5 T Magnet system

Methods to optimize an MgB$_2$ based conduction cooled MRI coil system has been elaborated in prior work [1]. Following these techniques, a ten coil system has been designed. TABLE contains dimensions for five of the bundles from the symmetric ten coil system. Bundle 5 is the shield coil that helps in confining the stray field between the 5 gauss line, the volume beyond which the magnetic field must be less than 5 gauss. The field inside the diameter spherical volume (DSV) is uniform on the order of 10 ppm. Each bundle is wound around a 10 mm thick mandrel with 10 mm thick sides made of Stainless Steel 302.

TABLE I
DESIGN DETAILS OF A 1.5 T CONDUCTION COOLED MRI MAGNET SYSTEM.

Coil	Inner Radius (m)	Outer Radius (m)	Starting Axial position (m)	Ending Axial Location (m)
Bundle 1	0.5001	0.5321	0.0496	0.1167
Bundle 2	0.5005	0.5327	0.2273	0.3181
Bundle 3	0.5000	0.5321	0.4639	0.5764
Bundle 4	0.5000	0.5321	0.6595	0.8699
Bundle 5	0.9059	0.9309	0.6122	0.8063
Current Density, J = 118.5A/mm^2				

B. Modeling of the composite wire and magnet system

The wire in consideration is an 18 filament MgB$_2$ wire shown in Fig. 1. The CAD model of the wire is prepared in the 3D modeling software Creo Parametric. One quarter of the
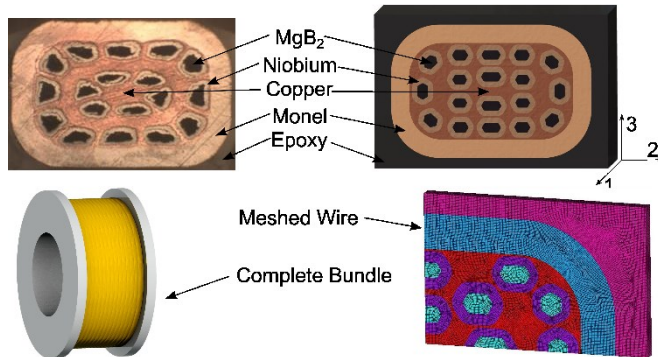

Fig. 1. 18 filament MgB$_2$ wire. Actual wire microscopic image on top left. CAD model of the wire, finite element mesh of the wire and complete bundle of the wire (Clockwise)

model is then imported into ANSYS, meshed accordingly with brick element SOLID 186. Suitable material properties are then assigned to the specified volume. A summary of the material properties are listed in TABLE . Methods to numerically homogenize the composite wire are elaborated by Barbero [24] and have been previously employed by Boso [25], [26] and Amin [12] for composite superconducting wire. A similar

TABLE II
SUMMARY OF THE MATERIAL PROPERTIES OF THE WIRE CONSTITUENTS

Material	Modulus of Elasticity (GPa) at 298 K	Poisson's ratio (v) at 298 K	Average thermal Expansion Coefficient (µm/m.K) (10~298 K)
MgB$_2$	273 [16]	0.181 [16]	4.23 [16]
Copper	129.5 [17]	0.355 [17]	10.9 [17]
Niobium	103 [18]	0.4 [18]	9.28 [19]
Monel	179 [20]	0.315 [20]	12.5 [20]
Glidcop® AL-60	130 [21]	0.32 [21]	16 [21]
Epoxy	12.9 [22]	0.355 [23]	19.83(Through Thickness), 6.23 (Warp or Fill) [22]
Stainless steel 302	190 [23]	0.305 [23]	12 [23]

approach is taken to numerically homogenize both the elastic properties and thermal expansion coefficient properties of the composite wire and are summarized on Table . These properties are used in the FEA model to compute the stress and strain development during winding, cool-down and electromagnetic charging.

C. Support conditions

At the time of winding— four different types of support on the mandrel can be used. No mandrel support during winding allows the mandrel to deform inwardly due to the applied

Table III
NUMERICALLY HOMOGENIZED MATERIAL PROPERTIES OF THE COMPOSITE SUPERCONDUCTOR.

Material Property (Directions are shown in Fig. 1)	Homogenized wire
Modulus of Elasticity (Direction 1)	112 GPa
Modulus of Elasticity (Direction 2)	57.9 GPa
Modulus of Elasticity (Direction 3)	59.6 GPa
Shear Modulus (Plane 1-2)	17.5 GPa
Shear Modulus (Plane 2-3)	13.4 GPa
Shear Modulus (Plane 3-1)	18 GPa
Poisson's ratio (Plane 1-2)	0.26
Poisson's ratio (Plane 2-3)	0.288
Poisson's ratio (Plane 3-1)	0.255
Avg. thermal expansion coefficient(direction. α_1)	10.1 µm/m-K
Avg. thermal expansion coefficient (direction α_2)	12.9 µm/m-K
Avg. thermal expansion coefficient (direction α_3)	12.6 µm/m-K

pretension on the wire (Case I). Only the radial support at the inner radial location of the mandrel restricts all inward deformation of the mandrel (Case II: radial displacement, $u_r = 0$). The combination of radial support and axial support restricts the deformation of the mandrel in both the radial and axial directions (Case III: radial displacement, u_r = axial displacement, $u_z = 0$). Only the axial support at the two extreme axial location of the mandrel restricts any axial deformation of the mandrel but allows any deformation inward in the radial location (Case IV: *axial displacement, $u_z = 0$*). After the winding is complete, all the supports are removed and the coil is thermally cooled down to 10 K and electromagnetically charged to a 1.5 T magnetic field.

III. RESULTS

The entire magnet system is solved utilizing a multiscale multiphysics FEA method as detailed in a prior article [12]. The principal strains represent a composite failure criteria more
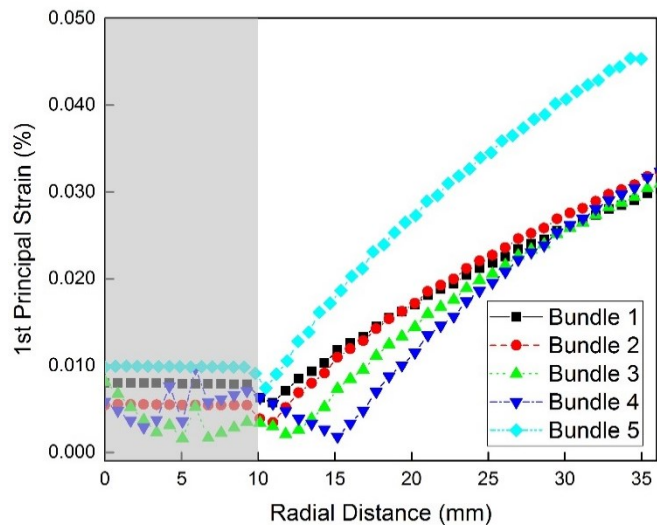

Fig. 2. 1st principal strain on all five bundles of the 1.5 T magnet system. Mandrel regions are shaded in gray. The plot is at the mid-plane from the mandrel inner surface to the outermost radial location of the bundles.

accurately [27] rather than the von Mises criteria and should be the primary concern. Also, the composite MgB_2 superconducting wire fails at 0.4% tensile strain under uniaxial tensile loading as demonstrated experimentally [2]–[5]. Hence, fig. 2 shows the 1st principal strain development in all of the
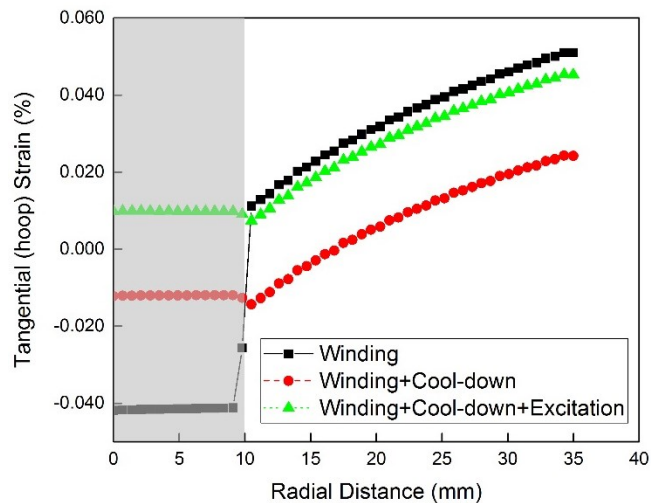

Fig. 3. Tangential strain development on bundle 5 at the end of each step.

five bundles after the winding is complete. There was no mandrel support in the radial direction for this case. From this figure, maximum strain development is observed in bundle 5 (shield coil). Therefore, considering only bundle 5 would be enough to picture the overall scenario of maximum strain development. The coil bundles undergo different processes—winding, cool-down and electromagnetic charging (excitation) and accumulates strain throughout these processes. Fig. 3 shows tangential (hoop) strain development on bundle 5. Tangential strain is plotted in this case because this strain helps

to understand the strain change with ease across different processes: winding, cool-down and electromagnetic charging. Form the figure, it is observed that the bundles are under tensile strain. As the system is cooled down to 10 K operating temperature, the strain drops and part of the bundle is now under compressive strain. After excitation, the strain in the bundle increases and becomes tensile but stays well below engineering
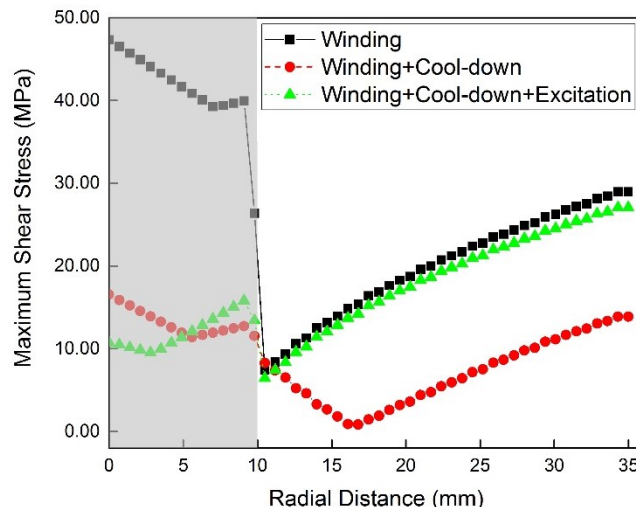

Fig. 4. Maximum shear stress in bundle 5 at different steps of manufacturing and operations.

design strain limit of 0.2% (half of the 0.4% irreversible strain).

During winding, if the floating coil technique is employed, the mandrel and coil bundle stay free of each other. Implementation of this winding technology facilitates the free movement of the bundle when the magnet is excited. However, conduction-cooled magnet would experience degradation in heat transfer and affect the cooling system attributed to decreased contact conductance if floating coil technique is employed. Hence, the mandrel and bundles are attached to each
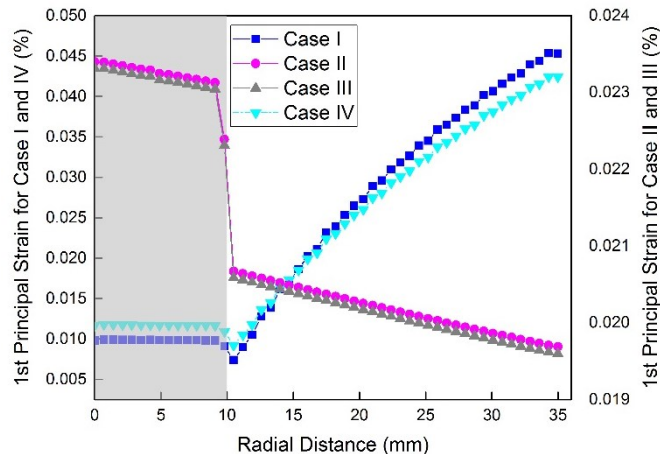

Fig. 5. 1st principals strain due to different winding support cases after the magnets are charged to 1.5 T field

other in this case. Maximum shear stress along the mid-plane from inner to outer radial locations is plotted in fig. 4 to understand the failure in the epoxy. A maximum shear stress of 28 MPa is observed at the outer surface of the bundle. The shear strength of epoxy at 4 K is 232 MPa [28]. The developed shear stress is well within the range of the failure strength of epoxy

and hence indicates a safe operation of the magnet system.

Four different boundary conditions has been employed during the winding process and subsequently removed prior to the cool-down and electromagnetic charging. The boundary
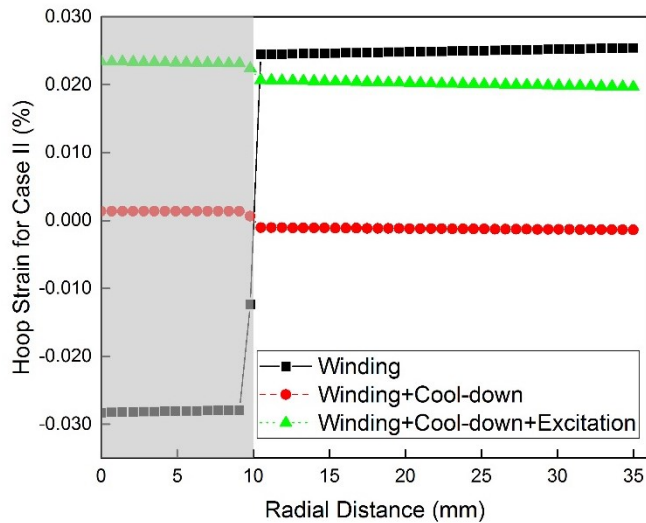

Fig. 6. Hoop strain on bundle 5 with case II

conditions are described previously in the section 'Support conditions' and the 1st principal strain development after electromagnetic charging is plotted in fig. 5. In case of no radial support on the mandrel, the mandrel and bundle both are allowed to deform inwardly due to the applied compressive stress by the pretension (31.14 MPa) [12] on the wire. This inward deformation assists in stress relaxation in the tangential direction and helps reduce the tensile stress in the lower layers at the time of winding as shown in fig 3. The tangential stresses are the most dominant stress components, and constitutes the majority of the 1st principal strain. Therefore, the 1st principal
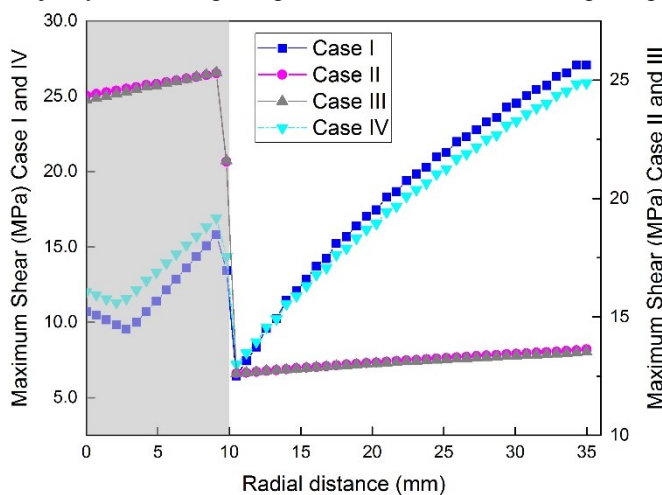

Fig. 7. Maximum shear stress on bundle 5 during electromagnetic excitation.

strain closely follows the trend of tangential strain. For case IV, the mandrel is supported in the axial direction. Hence, the 1st principal strain is similar to case I.

However, when case II and case III are employed, the deformation of the mandrel is restricted in the inward radial direction. This restriction allows the tangential stress to stay almost constant through the bundle along the radial direction.

During cooldown, the stresses reduce as the mandrel shrinks more in comparison to the bundle. This shrinkage allows extra space for the bundle to relax as the strain developed. As a result, from fig. 6, it is observed that the strain values drop after cooldown process. When the bundles are charged with the excitation current, they expand radially outward due to the Lorentz force. Again, as the inner surface of the mandrel is supported with constraints, most stress development occurs in the mandrel. As a result, higher strain development is observed in the mandrel while strain in the bundle is comparatively smaller. In a similar fashion, when case III is used, strain development is maximum in the mandrel while strains in the bundle stays low with a decreasing trend.

From fig. 5 when different boundary conditions are compared for the strain development, it appears that supporting the mandrel with radial support with axial support (Case III) is the most beneficial in terms of keeping the strains low. It is observed that not only the strain development is low but also the variation of the strain is narrow which is around 0.001% with a maximum strain occurring at the bundle-mandrel interface of 0.0207% to the outer most radial location of 0.0197%. This uniform strain development introduces a stabilization factor to the design that would help during quench induced strain due to hot spot.

Along with the strain development in the bundle, epoxy cracking is another major concern to design the magnet [9]. In order to check the integrity of the magnet bundle, maximum shear stress is also plotted for different support conditions. Again from fig. 7 it is clear that the shear stress is smaller in the bundle (~13 MPa) when support condition II or III is employed. This is about 12 MPa lower than support condition I and IV. Hence, it is suggested that the use of radial support along with axial support during wire winding minimizes the strain and shear stress development.

IV. CONCLUSION

Four different types of support conditions are investigated using the multiscale multiphysics FEA method to study the effect of strain and shear stress development on the coil bundles. In order to maintain a low strain and shear stress, supporting the mandrel radially along with axial support on the axial locations of the mandrel is beneficial over no radial support when a stainless steel mandrel is used for an 18 filament MgB_2 composite superconducting wire.

REFERENCES

[1]   T. Baig, Z. Yao, D. Doll, M. Tomsic, and M. Martens, "Conduction cooled magnet design for 1.5 T, 3.0 T and 7.0 T MRI systems," *Supercond. Sci. Technol.*, vol. 27, no. 12, p. 125012, Dec. 2014.
[2]   P. Kováč, L. Kopera, T. Melišek, M. Rindfleisch, W. Haessler, and I. Hušek, "Behaviour of filamentary MgB_2 wires subjected to tensile

stress at 4.2 K," *Supercond. Sci. Technol.*, vol. 26, no. 10, p. 105028, Oct. 2013.

[3] C. Zhou, P. Gao, H. J. G. Krooshoop, M. Dhallé, M. D. Sumption, M. Rindfleisch, M. Tomsic, M. Kulich, C. Senatore, and A. Nijhuis, "Intrawire resistance, AC loss and strain dependence of critical current in MgB2 wires with and without cold high-pressure densification," *Supercond. Sci. Technol.*, vol. 27, no. 7, p. 75002, Jul. 2014.

[4] H. Kitaguchi and H. Kumakura, "Superconducting and mechanical performance and the strain effects of a multifilamentary MgB_2/Ni tape," *Supercond. Sci. Technol.*, vol. 18, no. 12, p. S284, Dec. 2005.

[5] M. Dhallé, H. van Weeren, S. Wessel, A. den Ouden, H. H. J. ten Kate, I. Hušek, P. Kováč, S. Schlachter, and W. Goldacker, "Scaling the reversible strain response of MgB_2 conductors," *Supercond. Sci. Technol.*, vol. 18, no. 12, p. S253, Dec. 2005.

[6] J. Ekin, "Mechanisms for critical-current degradation in NbTi and Nb3Sn multifilamentary wires," *IEEE Trans. Magn.*, vol. 13, no. 1, pp. 127–130, Jan. 1977.

[7] L. Li, Z. Ni, J. Cheng, H. Wang, Q. Wang, and B. Zhao, "Effect of Pretension, Support Condition, and Cool Down on Mechanical Disturbance of Superconducting Coils," *IEEE Trans. Appl. Supercond.*, vol. 22, no. 2, pp. 3800104–3800104, Apr. 2012.

[8] E. S. Bobrov, J. E. C. Williams, and Y. Iwasa, "Experimental and theoretical investigation of mechanical disturbances in epoxy-impregnated superconducting coils. 2. Shear-stress-induced epoxy fracture as the principal source of premature quenches and training theoretical analysis," *Cryogenics*, vol. 25, no. 6, pp. 307–316, Jun. 1985.

[9] Y. Iwasa, "Mechanical disturbances in superconducting magnets-a review," *IEEE Trans. Magn.*, vol. 28, no. 1, pp. 113–120, Jan. 1992.

[10] L. Li, J. Cheng, Z. Ni, H. Wang, Y. Dai, and Q. Wang, "Preliminary Mechanical Analysis of a 9.4-T Whole-Body MRI Magnet," *IEEE Trans. Appl. Supercond.*, vol. 25, no. 2, pp. 1–7, Apr. 2015.

[11] C. Poole, T. Baig, R. J. Deissler, D. Doll, M. Tomsic, and M. Martens, "Numerical study on the quench propagation in a 1.5 T MgB_2 MRI magnet design with varied wire compositions," *Supercond. Sci. Technol.*, vol. 29, no. 4, p. 44003, Apr. 2016.

[12] A. A. Amin, T. Baig, R. J. Deissler, Z. Yao, M. Tomsic, D. Doll, O. Akkus, and M. Martens, "A multiscale and multiphysics model of strain development in a 1.5 T MRI magnet designed with 36 filament composite MgB_2 superconducting wire," *Supercond. Sci. Technol.*, vol. 29, no. 5, p. 55008, May 2016.

[13] R. J. Deissler, T. Baig, C. Poole, A. Amin, D. Doll, M. Tomsic, and M. Martens, "Numerical Simulation of Quench Protection for a 1.5 T Persistent-Mode MgB2 Conduction-Cooled MRI Magnet.," *Supercond. Sci. Technol.*, vol. submitted for publication, May 2016.

[14] A. Amin, T. N. Baig, Z. Yao, and M. Martens, "Stress and Strain Sensitivity Study of 1.5T Conduction Cooled MgB2 Magnet Design," presented at the International Society for Magnetic Resonance in Medicine, Toronto, ON, 2015.

[15] T. A. Prikhna, "Properties of MgB_2 bulk," *ArXiv Prepr. ArXiv09124906*, 2009.

[16] J. J. Neumeier, T. Tomita, M. Debessai, J. S. Schilling, P. W. Barnes, D. G. Hinks, and J. D. Jorgensen, "Negative thermal expansion of Mg B 2 in the superconducting state and anomalous behavior of the bulk Grüneisen function," *Phys. Rev. B*, vol. 72, no. 22, p. 220505, 2005.

[17] http://www.copper.org/resources/properties/cryogenic/, .

[18] https://en.wikipedia.org/wiki/Niobium, .

[19] G. K. White, "Thermal expansion of vanadium, niobium, and tantalum at low temperatures," *Cryogenics*, vol. 2, no. 5, pp. 292–296, Sep. 1962.

[20] http://www.specialmetals.com/assets/documents/alloys/monel/monel-alloy-400.pdf, .

[21] "Glidcop copper dispersion strengthened with aluminum oxize." Argonne National laboratory.

[22] http://ncsx.pppl.gov/NCSX_Engineering/Materials/InsulationProperties/CTD-101K_Datasheet_2003.pdf, .

[23] J. E. Jensen, R. G. Stewart, W. A. Tuttle, and H. Brechna, *Brookhaven National Laboratory Selected Cryogenic Data Notebook: Sections X-XVIII*, vol. 2. Brookhaven National Laboratory, 1980.

[24] E. J. Barbero, *Finite Element Analysis of Composite Materials Using ANSYS®, Second Edition*. CRC Press, 2013.

[25] D. P. Boso, "A simple and effective approach for thermo-mechanical modelling of composite superconducting wires," *Supercond. Sci. Technol.*, vol. 26, no. 4, p. 45006, 2013.

[26] D. P. Boso, M. Lefik, and B. A. Schrefler, "Homogenisation methods for the thermo-mechanical analysis of Nb3Sn strand," *Cryogenics*, vol. 46, no. 7–8, pp. 569–580, Jul. 2006.

[27] A. C. Orifici, I. Herszberg, and R. S. Thomson, "Review of methodologies for composite material modelling incorporating failure," *Compos. Struct.*, vol. 86, no. 1–3, pp. 194–210, Nov. 2008.

[28] N. A. Munshi and H. W. Weber, "Reactor Neutron and Gamma Irradiation of Various Composite Materials," in *Materials*, F. R. Fickett and R. P. Reed, Eds. Springer US, 1992, pp. 233–239.